

Article

Density Measurements of Waste Cooking Oil Biodiesel and Diesel Blends Over Extended Pressure and Temperature Ranges

Thanh Xuan NguyenThi ¹ , Jean-Patrick Bazile ² and David Bessières ^{2,*}

¹ Department of Chemical Engineering—Petroleum and Gas, The University of Danang—University of Science and Technology, 54 Nguyen Luong Bang, DaNang 550000, Vietnam; ntxuan@dut.udn.vn

² TOTAL-Laboratoire des Fluides Complexes et leurs Réservoirs, University Pau & Pays Adour, UMR 5150–LFC–R, CNRS, BP 1155–Pau, F-64013, France; jean-patrick.bazile@univ-pau.fr

* Correspondence: david.bessieres@univ-pau.fr

Received: 13 April 2018; Accepted: 7 May 2018; Published: 9 May 2018



Abstract: Density and compressibility are primordial parameters for the optimization of diesel engine operation. With this objective, these properties were reported for waste cooking oil biodiesel and its blends (5% and 10% by volume) mixed with diesel. The density measurements were performed over expanded ranges of pressure (0.1 to 140 MPa) and temperature (293.15 to 353.15 K) compatible with engine applications. The isothermal compressibility was estimated within the same experimental range by density differentiation. The Fatty Acid Methyl Esters (FAMES) profile of the biodiesel was determined using a Gas Chromatography–Mass Spectrometry (GC–MS) technique. The storage stability of the biodiesel was assessed in terms of the reproducibility of the measured properties. The transferability of this biodiesel fuel was discussed on the basis of the standards specifications that support their use in fuel engines. Additionally, this original set of data represents meaningful information to develop new approaches or to evaluate the predictive capability of models previously developed.

Keywords: waste cooking oil biodiesel; FAMES profile; storage stability; density; viscosity

1. Introduction

Biodiesel, known as a renewable and environmentally friendly fuel, has attracted the attention of the scientific community over the past decade. Feedstocks for biodiesel production have been studied over three generations. The first generation deals with vegetable oils—traditional edible oil, which may cause the problem of food shortages and agricultural land competition. The debate on the sustainability of this first-generation biodiesel has led to the research of second- and third-generation biodiesels [1]. The second generation of biodiesel consists of agricultural byproducts, waste oil, and animal fats. These are considered to be a promising alternative source for edible plants and in line with each country's regional development strategy [2,3]. This work implemented the second-generation biodiesel issue of waste cooking oil to be used as biodiesel feedstocks. Waste cooking oil (WCO) is a fatty waste from food processing and is no longer suitable for human use. The massive development of tourism services along with food processing chains, especially fast-food chains, and the rise of instant noodle factories in developing countries has led to the discharge of large amounts of WCO. This is becoming a serious environmental problem. WCO released directly into sewage pipes will cause congestion in sewer lines; when entering sewage treatment plants, it generates operational troubles or system overloading because lipids are very difficult to decompose, and are therefore causes of soil and water pollution [4]. Many recent studies on biodiesel production from WCO have revealed the great potential of this feedstock compared with first-generation biodiesel in terms of resolving environmental, economic, and social issues simultaneously [5–10].

Considering energy and environmental issues, one of the most important concerns is the fuel injection system which operates at high pressure. The objective here is to introduce the appropriate amount of fuel into the engine in order to enhance the fuel/air mixture combustion [11] for engine efficiency. Calibrated high-pressure injection supposes an accurate knowledge of the thermophysical properties of biodiesel over wide ranges of pressure and temperature. Among them, density is an important parameter that influences the conversion of volume flow rate into mass biodiesel flow rate [12], whereas the compressibility linked to a bulk modulus controls the fuel injection timing [13]. Their knowledge is of importance within the same operating pressure and temperature ranges.

In this context, the present work aims to provide a complete thermophysical characterization of a biodiesel produced from WCO which was procured from a local restaurant in Vietnam. The Fatty Acid Methyl Esters (FAMEs) profile of this biodiesel sample was determined through the use of a GC-MS technique. Additionally, two different fuel blends (5%, 10% by volume mixing with base diesel) were studied along with base diesel fuel and pure biodiesel. The diesel was provided by a refinery. The choice of these compositions meets the most common commercial blends today in use. Density measurements were performed for the pure biodiesel and its two blends within broad ranges of pressure (0.1 to 140 MPa) and temperature (293.15 to 353.15 K) which meet the operating conditions in engine use. The differentiation of the density measurement allows estimation of the isothermal compressibility in the same pressure and temperature ranges. The reproducibility of the two properties was checked for each sample. This is also an unambiguous indicator of the storage stability of the biodiesel. The paper is organized as follows. Section 2 details the description of the experimental techniques, whereas Section 3 reports all results obtained for the thermophysical properties as well as information on the materials' composition. The potential use of this fluid as biodiesel is discussed on the basis of this experimental study.

2. Experimental Techniques

2.1. WCO Biodiesel Preparation and FAME Analysis Method

2.1.1. WCO Biodiesel Synthesis

The WCO used as a feedstock for biodiesel synthesis in this study was procured from a local restaurant in Vietnam. The WCO sample was obtained by the way of collection after being used once for cooking various dishes and then filtered to remove any inorganic residues and suspended matter. The first phase of the study concerned the analysis of the WCO sample. Some of its chemical properties—saponification value, acid value, and Iodine number—were determined as 192.64 mg KOH/g, 3.96 mg KOH/g, and 87.76 g I₂/100g, respectively (Table 1).

Table 1. Main properties of the analyzed WCO.

Property	Units	Average Value
Saponification value	mg KOH/g	192.64
Acid value	mg KOH/g	3.96
Iodine number	g I ₂ /100g	87.76

Taking into consideration the average acid value of 3.96 mg KOH/g, corresponding to the weight percent of Free Fatty Acid (%FFA) lower than 2%, the methods used for biodiesel production from WCO are very similar to the conventional transesterification process with an alkali catalyst. The transesterification procedure was carried out following the steps detailed in the research of Basak Burcu Uzun et al. [14] at optimized conditions such as a methanol/oil molar ratio of 7:1, a reaction time of 30 min, and a reaction temperature of 50 °C in the presence of NaOH catalyst at a concentration of 0.5 wt %. At the end of the reaction, the product mixture was poured into a separating funnel, and left overnight to cool down and for separation of phases. After removing the

lower phase which contained the glycerol, remaining catalyst, extra methanol, and undesired products, we received the upper phase consisting of methyl esters and lower concentrations of catalyst, glycerol, and methanol. This ester layer was washed several times with a small amount of hot distilled water each time until the washings were neutral. The washed methyl esters were then dried under vacuum and weighed to find the biodiesel yields.

2.1.2. FAMES Analysis

The FAMES in biodiesel prepared from WCO were estimated using a Thermo Scientific™ ISQ™ LT Single Quadrupole GC-MS System (Thermo Fisher Scientific, Waltham, MA, USA). The column used was a Thermo Scientific™ Trace GOLD TG-5MS Column with dimensions of 0.25 μm thickness, 0.25 mm ID, 30 m length. This Thermo Scientific TraceGOLD TG-5MS column is a low-polarity, 5% diphenyl/95% dimethyl polysiloxane column which is ideal for most Gas Chromatography applications. This phase gives extremely low bleed and has a maximum operating temperature of 350 °C. The oven temperature was initially held at 160 °C for 2 min, increased to 180 °C at 2 °C/min and held for 2 min, increased continuously to 250 °C at 10 °C/min, and then held for 2 min. The injector, transfer, and source temperatures were 250 °C, 260 °C, and 240 °C, respectively. The carrier gas was helium and the total scan time was 24 min. The EI mode of ionization was applied and the mass scan range was from 50 to 450 m/z. GC-MS solution Xcalibur software was used for data processing. For identification of FAMES, a library search was carried out using National Institute of Standards and Technology (NIST), National Bureau of Standards (NBS), and Wiley GC-MS libraries. The individual peaks of the gas chromatogram were analyzed and the fatty acids were identified using the MS database. The relative percentage of fatty acid esters was calculated from total ion chromatography by a computerized integrator.

2.2. High-Pressure Density Measurement

Density was measured as a function of pressure and temperature using an ANTON-PAAR vibrating tube densimeter (Anton Paar GmbH, Graz, Austria) equipped with a high-pressure cell (DMA HPM). This high-pressure densimeter cell enables measurements over broad ranges of pressure (0.1 to 140 MPa) and temperature (283.15 to 403.15 K). The well-known measurement principle consists of determining the oscillation period of a U-shaped tube which contains the sample. The square of this period is correlated to the density through a linear relationship. The parameters of this linear law were determined using water and decane as a reference liquid. This calibration procedure has been largely detailed elsewhere. For examples, see the works of Lagourette et.al. [15], Miyake et.al. [16], and Pineiro et.al. [17]. The estimated uncertainty of the measured temperature is ± 0.01 K between (293.15 and 353.15 K) (Anton Paar MKT50 thermometer) while the estimated uncertainty of the measured pressure is ± 0.015 MPa (Presents Precise Gold Plus pressure transmitter); as a consequence, the uncertainty on the density measurement is estimated to be ± 0.5 kg m^{-3} (i.e., around 0.05% for density close to that of water). This uncertainty is similar to that reported in several other studies [14–17].

3. Results and Discussion

3.1. Fresh Biodiesel: Relative Compositions of Fatty Acid Contents

The fatty acid profile of the biodiesel prepared from waste cooking oil is presented in Figure 1.

The relative percentage of fatty acid esters was calculated from total ion chromatography by a computerized integrator, and the results are presented in Table 2.

Oleic acid (C18:1) and palmitic acid (C16:0) are the major fatty acids in WCO biodiesel with 37.59 wt % and 25.14 wt %, respectively, followed by stearate acid (C18:0, 13.18 wt %), linoleic acid (C18:2, 9.76 wt %), and palmitoleic acid (C16:1, 7.16 wt %). The long-chain fatty acids are present as minor constituents. This result conforms with those of the investigation conducted by Leung and Guo [18]

who synthesized biodiesel from used frying oil collected from local Chinese restaurants. The study by Huseyin Sanli et al. [19] conducted on 35 samples taken from different facilities producing waste frying oils (fast foods, fish restaurants, and hospital restaurants) resulted in equivalent FAMES profiles, especially for the samples from fast foods and fish restaurants. Their FAME analysis showed that the fatty acids of these biodiesels were composed primarily of oleic acid and palmitic acid, followed by linoleic acid. These components are able to improve not only certain important fuel properties like cetane number, heat of combustion, oxidative stability, and kinematic viscosity (C18:1, C16:0), but also the cold flow properties of biodiesel (C18:2) as shown in the works of Knothe G. [20] Based on this profile of fatty acid composition, it is clearly assumed that waste cooking oil is suitable for biodiesel production. The storage stability of the sample was then checked.

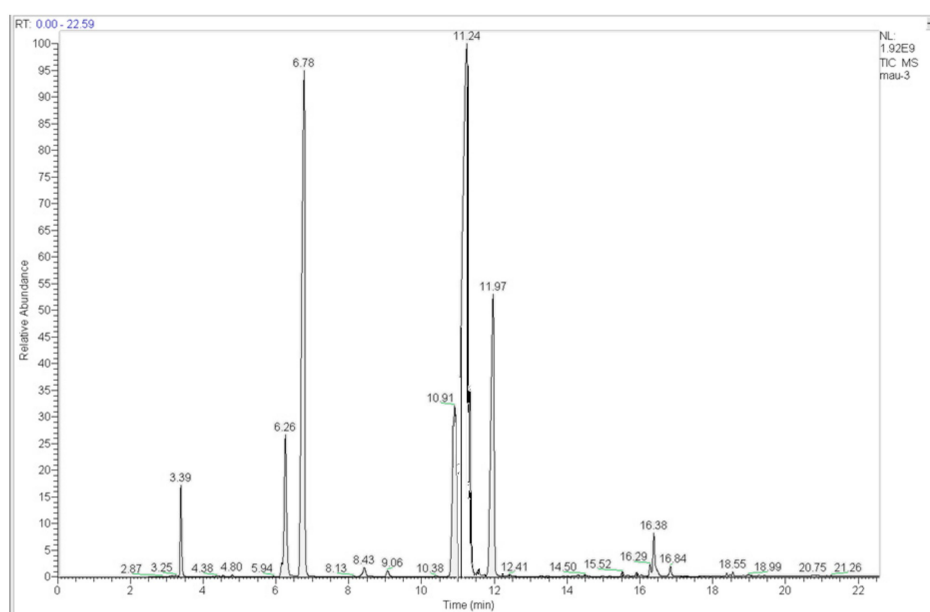


Figure 1. Gas chromatogram of biodiesel from waste cooking oil.

Table 2. Fatty Acid Methyl Ester (FAME) profile of the WCO biodiesel (in terms of relative weight percentage).

Retention Time (min)	FAME	wt %
3.39	Methyl myristate (C14:0)	3.22
6.26	Methyl palmitoleate (C16:1)	7.16
6.78	Methyl palmitate (C16:0)	25.14
10.91	Methyl linoleate (C18:2)	9.76
11.24	Methyl oleate (C18:1)	37.59
11.97	Methyl stearate (C18:0)	13.18
16.29	Methyl eicosadienoate (C20:2)	0.53
16.38	Methyl eicosenoate (C20:1)	1.77
16.84	Methyl eicosanoate (C20:0)	0.62

Previous to any experimental measurement, the stability of the fresh biodiesel sample was checked. In this study, the oxidative or storage stability was assessed through the reproducibility of the density and viscosity measurements, knowing that such properties are clearly affected by a modification of the FAMES profile due to oxidation processes. The methodology followed here consists of replicating density measurements at 0, 8, 12, and 24 weeks. For both properties, the reproducibility observed was within the allowed uncertainty range, thus supporting the transferability of the biodiesel. Note that the oxidative stability of a biodiesel produced from waste fish oil was extensively studied in a recent work reported in the literature [21].

3.2. Density Measurements

Density measurements were carried out along various isotherms spaced at 20 K intervals (from 293.15 to 353.15 K) and for pressures (ranging from 0.1 to 140 MPa) in steps of 10 MPa. This experimental range was fully described without the appearance of solid deposition which is a good indicator in terms of the cold properties of this biodiesel. The original experimental density data are listed in Table 3 for the waste cooking oil biodiesel (B100) and its blends with diesel containing 5 and 10 vol % biodiesel, named B5 and B10, respectively. We recall that the uncertainty is estimated to be $0.5 \times 10^{-3} \text{ g/cm}^3$. In this study we are interested in the blends of 5 and 10 vol % biodiesel based on Vietnam's fuel use.

Table 3. Experimental densities, ρ , of WCO biodiesel (B100) and pure diesel (B0) as well as the blends of biodiesel and diesel (B5 and B10) at various temperatures T and pressures P.

P (MPa)	T (K)			
	293.15	313.15	333.15	353.15
$\rho \text{ (g}\cdot\text{cm}^{-3}\text{)}$				
B100				
0.1	0.9164	0.9022	0.8891	0.8755
10	0.9216	0.9078	0.8952	0.8824
20	0.9266	0.9127	0.9012	0.8888
30	0.9314	0.9183	0.9065	0.8948
40	0.9359	0.9232	0.9117	0.9002
50	0.9403	0.9279	0.9165	0.9054
60	0.9444	0.9322	0.9212	0.9103
70	0.9485	0.9365	0.9258	0.9149
80	0.9523	0.9407	0.9300	0.9195
90	0.9560	0.9445	0.9342	0.9238
100	0.9601	0.9485	0.9381	0.9281
110	0.9642	0.9520	0.9419	0.9320
120	0.9682	0.9554	0.9456	0.9359
130	0.9721	0.9588	0.9491	0.9396
140	0.9760	0.9621	0.9526	0.9431
B0				
0.1	0.8325	0.8183	0.8044	0.7897
10	0.8388	0.8250	0.8117	0.7982
20	0.8444	0.8312	0.8185	0.8057
30	0.8498	0.8371	0.8250	0.8127
40	0.8548	0.8425	0.8309	0.8191
50	0.8596	0.8475	0.8366	0.8250
60	0.8640	0.8525	0.8417	0.8304
70	0.8683	0.8570	0.8466	0.8356
80	0.8724	0.8614	0.8510	0.8404
90	0.8763	0.8657	0.8555	0.8452
100	0.8801	0.8698	0.8598	0.8497
110	0.8837	0.8737	0.8639	0.8539
120	0.8875	0.8773	0.8678	0.8580
130	0.8908	0.8807	0.8716	0.8621
140	0.8942	0.8842	0.8751	0.8658
B5				
0.1	0.8368	0.8225	0.8089	0.7943
10	0.8427	0.8290	0.8161	0.8024
20	0.8484	0.8353	0.8228	0.8100
30	0.8538	0.8410	0.8290	0.8169
40	0.8587	0.8465	0.8349	0.8231
50	0.8634	0.8516	0.8405	0.8290

Table 3. Cont.

P (MPa)	T (K)			
	293.15	313.15	333.15	353.15
	ρ (g·cm ⁻³)			
60	0.8679	0.8564	0.8457	0.8346
70	0.8722	0.8609	0.8505	0.8397
80	0.8764	0.8654	0.8550	0.8446
90	0.8804	0.8696	0.8595	0.8493
100	0.8844	0.8736	0.8638	0.8538
110	0.8878	0.8774	0.8679	0.8579
120	0.8911	0.8812	0.8719	0.8621
130	0.8947	0.8847	0.8756	0.8661
140	0.8980	0.8882	0.8791	0.8698
	B10			
0.1	0.8413	0.8268	0.8132	0.7989
10	0.8471	0.8333	0.8203	0.8069
20	0.8528	0.8395	0.8271	0.8141
30	0.8580	0.8452	0.8333	0.8211
40	0.8629	0.8506	0.8392	0.8272
50	0.8676	0.8557	0.8446	0.8330
60	0.8721	0.8605	0.8497	0.8386
70	0.8764	0.8650	0.8545	0.8436
80	0.8805	0.8695	0.8592	0.8486
90	0.8844	0.8736	0.8638	0.8533
100	0.8881	0.8776	0.8679	0.8576
110	0.8918	0.8814	0.8719	0.8620
120	0.8955	0.8852	0.8758	0.8661
130	0.8989	0.8888	0.8795	0.8699
140	0.9023	0.8922	0.8832	0.8737

Figure 2 displays the pure biodiesel density as a function of pressure (isothermal curves), whereas in Figure 3 is plotted the variation of density as a function of temperature (isobaric curves). The value of the density extrapolated at 288.15 K and atmospheric pressure is 0.9192 g/cm³, which is somewhat higher than that the value of the EN 14214 specifications (upper limit 0.9000 g/cm³), which is one of the standards used.

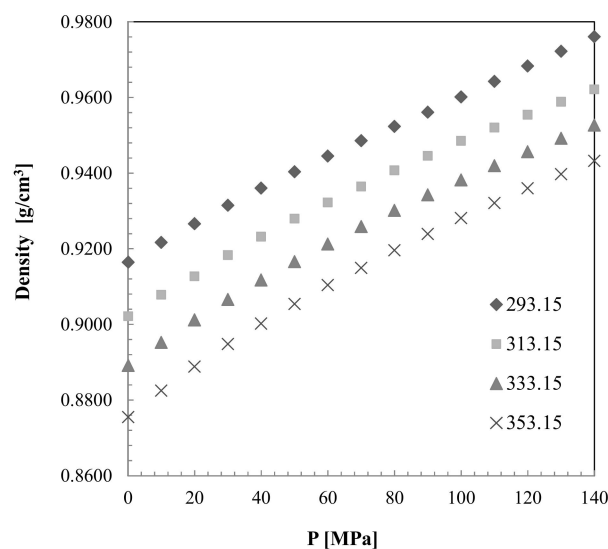


Figure 2. Variation of the WCO biodiesel density as a function of pressure at different temperatures: \blacklozenge 293.15 K, \blacksquare 313.15 K, \blacktriangle 333.15 K, \times 353.15 K.

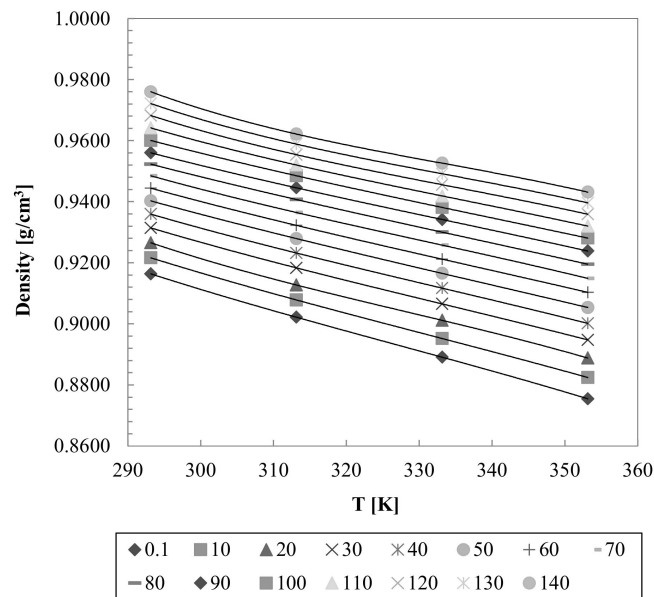


Figure 3. Variation of the fresh biodiesel density as a function of temperature at different pressures (0.1 to 140 MPa). (Lines are visual guides.)

Experimental results of the density of biodiesel and its blends with diesel have been plotted in Figure 4 for varying pressure (isothermal curves) at 293.15 K and in Figure 5 for varying temperature at atmospheric pressure (0.1 MPa). It was found that at a particular pressure/temperature, the lower blend ratio in biodiesel results in lower densities. The diesel is a standard diesel for which the density value is 0.8325 g/cm^3 at 293.15 K and atmospheric pressure. The density values are very similar to those advised by Ndiaye et al. [11] for a normal fluid designed for fuel engines.

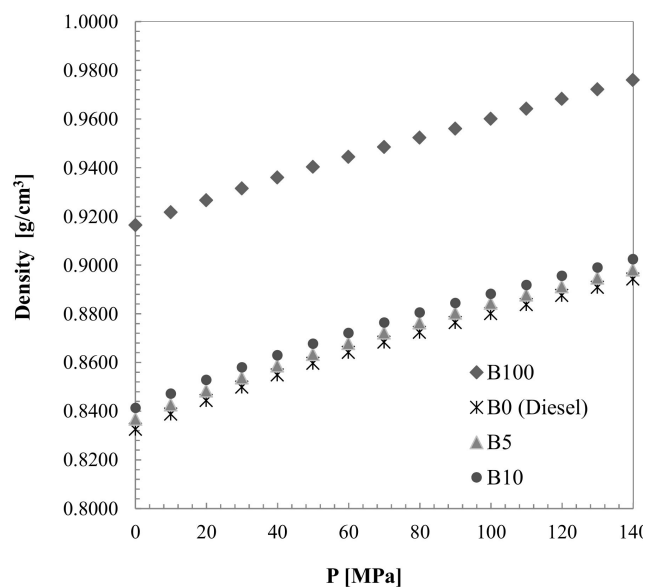


Figure 4. Experimental results of the density of WCO biodiesel (B100), pure diesel (B0), and their blends (B5, B10) for varying pressure (isothermal curves) at 293.15 K.

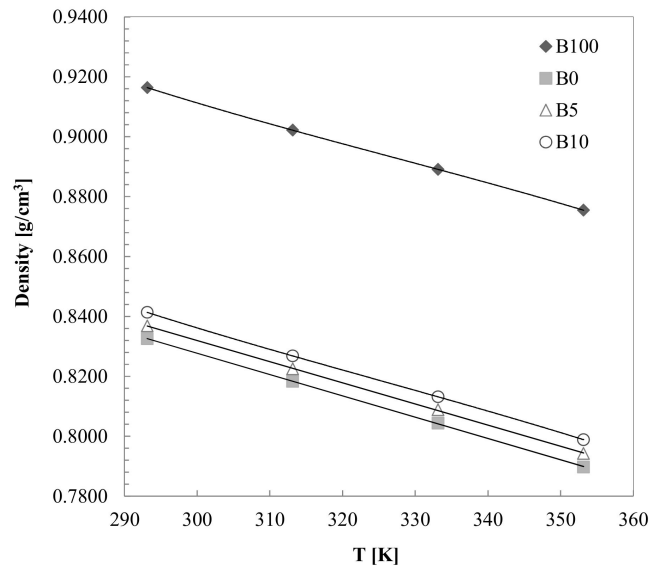


Figure 5. Experimental results of the density of WCO biodiesel (B100), pure diesel (B0), and their blends (B5, B10) for varying temperature (isobar curves) at atmospheric pressure (0.1 MPa).

A modified Tait-like equation was used in order to correlate the density over the entire pressure and temperature ranges:

$$\rho(P, T) = \frac{\rho_0(T)}{1 - C \ln \frac{P+B(T)}{0.1+B(T)}} \quad (1)$$

in which

$$\rho_0(T) = A_0 + A_1T + A_2T^2 + A_3T^3 \quad (2)$$

$$B(T) = B_0 + B_1T + B_2T^2 \quad (3)$$

Several indicators allow comparison of the experimental density values with those obtained with the Tait correlation. The absolute average deviation (AAD), the maximum deviation (DMax), the average deviation (Bias), and the standard deviation (σ) are defined as follows:

$$AAD = \frac{100}{N} \sum_{i=1}^N \left| \frac{\rho_i^{\text{exp}} - \rho_i^{\text{calc}}}{\rho_i^{\text{exp}}} \right| \quad (4)$$

$$DMax = \text{Max} \left(100 \left| \frac{\rho_i^{\text{exp}} - \rho_i^{\text{calc}}}{\rho_i^{\text{exp}}} \right| \right) \quad (5)$$

$$\text{Bias} = \frac{100}{N} \sum_{i=1}^N \frac{\rho_i^{\text{exp}} - \rho_i^{\text{calc}}}{\rho_i^{\text{exp}}} \quad (6)$$

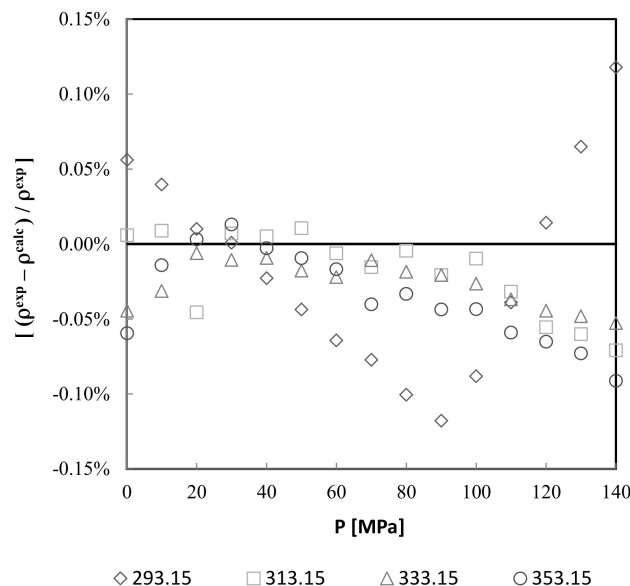
$$\sigma = \sqrt{\frac{\sum_{i=1}^N (\rho_i^{\text{exp}} - \rho_i^{\text{calc}})^2}{N - m}} \quad (7)$$

where N is the number of experimental data ($N = 60$ for each compound), m is the number of parameters ($m = 8$ in Equation (1)), and ρ_i^{exp} and ρ_i^{calc} are the experimental density values of this work and those obtained with Equation (1), respectively. The Tait correlation parameters, along with the AAD, DMax, Bias, and standard deviation σ , obtained with this correlation are given in Table 4 for the WCO biodiesel (B100), pure diesel (B0), and their blends (B5 and B10).

Table 4. Obtained parameters and deviations for density correlation by using the Tait equation for WCO biodiesel (B100), pure diesel (B0), and their blends (B5 and B10).

Coefficients	B100	B0	B5	B10
$A_0/\text{g}\cdot\text{cm}^{-3}$	2.519378	1.662832	1.710722	1.837863
$A_1/\text{g}\cdot\text{cm}^{-3}\cdot\text{K}^{-1}$	-0.013766	-0.006533	-0.006947	-0.008047
$A_2/\text{g}\cdot\text{cm}^{-3}\cdot\text{K}^{-2}$	4.0498×10^{-5}	1.8122×10^{-5}	1.9405×10^{-5}	2.2675×10^{-5}
$A_3/\text{g}\cdot\text{cm}^{-3}\cdot\text{K}^{-3}$	-4.1607×10^{-8}	-1.8749×10^{-8}	-2.0051×10^{-8}	-2.3271×10^{-8}
B_0/MPa	-22.687549	438.128864	432.078831	480.962920
$B_1/\text{MPa}\cdot\text{K}^{-1}$	1.523006	-1.576172	-1.509124	-1.786701
$B_2/\text{MPa}\cdot\text{K}^{-1}$	-0.003194	0.001556	0.001440	0.001858
C	0.091540	0.083663	0.084928	0.085788
$\sigma/\text{g}\cdot\text{cm}^{-3}$	0.000475	0.00011	0.00082	0.00084
AAD/%	0.03641%	0.00936%	0.00687%	0.00716%
Dmax/%	0.11784%	0.02608%	0.02830%	0.02683%
Bias/%	-0.02453%	0.00250%	0.00054%	-0.00098%

Figures 6 and 7 display the relative deviations between experimental data and calculated densities using the Tait equation as function of pressure for the WCO biodiesel at different temperatures (Figure 6) as well as for all samples at 293.15 K (Figure 7a) and 353.15 K (Figure 7b). A careful analysis of this set of data shows very good agreement between experimental values and values obtained from Equation (1) except for pressure ranging from 110 to 140 MPa at 293.15 K. In this specific zone, the deviation increases up to 0.15%, which is somewhat higher than the expected uncertainty. This is probably due to a significant increase in the viscosity of the biodiesel. Using the same technique as in this work, Segovia et al. [22] claim that the uncertainty depends on the experimental ranges, increasing up to $5 \text{ kg}\cdot\text{m}^{-3}$ for highly viscous fluids. Such an increase is explained by the damping effect on the densimeter cell. In the case of our study, the pattern of density is very consistent. We report all the data knowing that uncertainties in the density values for the highest pressures (110 to 140 MPa) at 293.15 K should be more elevated due to the viscosity effect.

**Figure 6.** Relative deviations between experimental data and calculated densities using the Tait equation as function of pressure at different temperatures for fresh biodiesel B100. The zero line is experimental data.

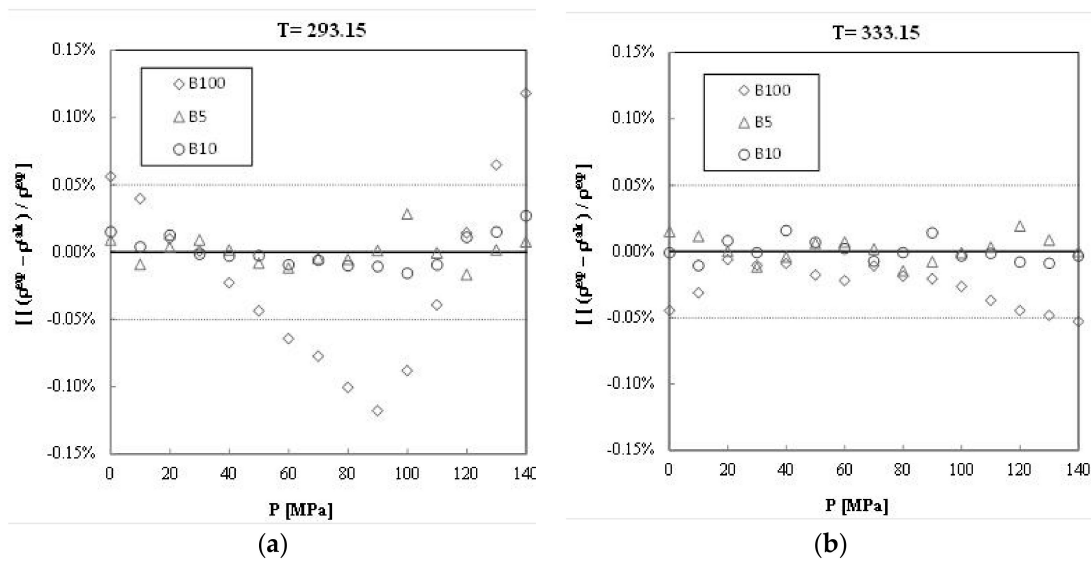


Figure 7. Relative deviations between experimental data and calculated densities using the Tait equation as a function of pressure at 293.15 K (a) and 333.15 K (b) for all samples. The zero line is experimental data.

3.3. Isothermal Compressibility

The isothermal compressibility is defined as:

$$\kappa_T = \frac{1}{\rho} \left(\frac{d\rho}{dP} \right)_T \quad (8)$$

The values are obtained by analytical differentiation with respect to pressure of Equation (1). Knowing that the original Tait equation is a phenomenological representation of the compressibility versus pressure, the values of κ_T were obtained by analytical differentiation of Equation (1). This is the most direct way to get reliable values of the isothermal compressibility. The uncertainty is estimated to be lower than 2%, as reported in previous studies [23,24]. As an illustration, in Figure 8 is plotted the variation of κ_T as a function of pressure (isothermal curves) for the biodiesel. Figure 9a,b display the variation of the isothermal compressibility for both the pure biodiesel and its blends.

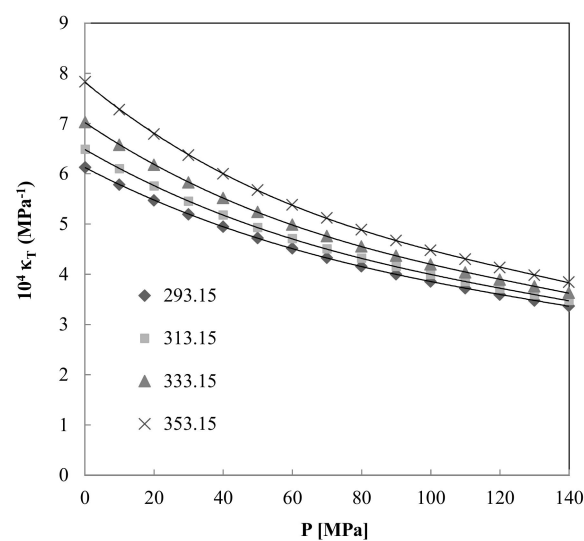


Figure 8. Variation of WCO biodiesel κ_T as a function of pressure for various temperatures: \blacklozenge 293.15 K, \blacksquare 313.15 K, \blacktriangle 333.15 K, \times 353.15 K.

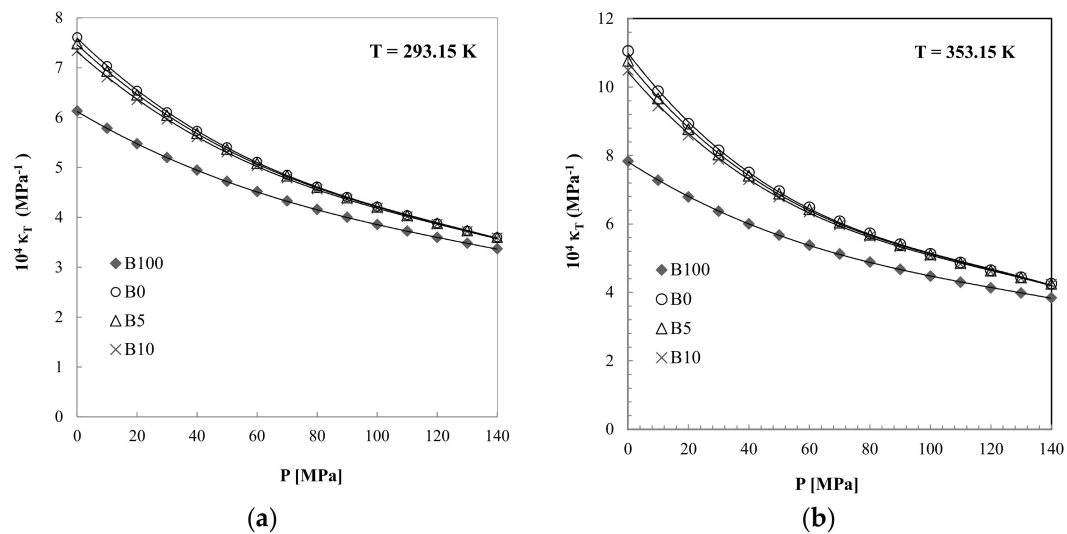


Figure 9. Variation of κ_T as a function of pressure of biodiesel (B100), pure diesel (B0), and their blends (B5 and B10) at 293.15 K (a) and at 353.15 K (b).

A very similar behavior is observed for all the samples. It tends to a constant and common value towards higher pressures. From a theoretical point of view, this behavior already reported should be regarded as a meaningful test to validate the development of models. It also represents useful information for testing and calibrating engine systems.

The raw data of the isothermal compressibility κ_T obtained for the biodiesel, diesel, and its blends (B5 and B10) are listed in Table 5.

Table 5. The raw data of κ_T obtained for the WCO biodiesel (B100), pure diesel (B0), and their blends (B5 and B10).

P (MPa)	T (K)			
	293.15	313.15	333.15	353.15
$10^4 \kappa_T$ (MPa $^{-1}$)				
B100				
0.1	6.12791	6.48718	7.02636	7.83080
10	5.78100	6.09975	6.57421	7.27352
20	5.47017	5.75489	6.17567	6.78935
30	5.19265	5.44879	5.82495	6.36858
40	4.94329	5.17517	5.51383	5.99938
50	4.71796	4.92906	5.23586	5.67269
60	4.51330	4.70645	4.98596	5.38148
70	4.32655	4.50409	4.76002	5.12019
80	4.15544	4.31930	4.55470	4.88437
90	3.99803	4.14986	4.36727	4.67043
100	3.85274	3.99390	4.19546	4.47542
110	3.71819	3.84985	4.03736	4.29688
120	3.59322	3.71638	3.89137	4.13280
130	3.47683	3.59235	3.75614	3.98146
140	3.36815	3.47678	3.63050	3.84141
B0				
0.1	7.61049	8.60011	9.74224	11.04942
10	7.03248	7.86956	8.81570	9.87327

Table 5. Cont.

P (MPa)	T (K)			
	293.15	313.15	333.15	353.15
	$10^4 \kappa_T$ (MPa ⁻¹)			
20	6.53495	7.25255	8.04977	8.92402
30	6.10605	6.72913	7.41149	8.14823
40	5.73233	6.27928	6.87108	7.50188
50	5.40366	5.88833	6.40738	6.95472
60	5.11228	5.54530	6.00497	6.48529
70	4.85210	5.24179	5.65232	6.07796
80	4.61831	4.97125	5.34061	5.72102
90	4.40703	4.72854	5.06304	5.40555
100	4.21513	4.50950	4.81421	5.12465
110	4.04002	4.31081	4.58983	4.87285
120	3.87957	4.12970	4.38642	4.64580
130	3.73198	3.96393	4.20113	4.43997
140	3.59574	3.81159	4.03161	4.25249
	B5			
0.1	7.47859	8.42162	9.51242	10.76818
10	6.92808	7.73026	8.64008	9.66432
20	6.45196	7.14291	7.91387	8.76612
30	6.03980	6.64217	7.30517	8.02721
40	5.67939	6.20998	6.78728	7.40824
50	5.36144	5.83303	6.34108	6.88188
60	5.07879	5.50122	5.95247	6.42856
70	4.82579	5.20682	5.61085	6.03390
80	4.59795	4.94376	5.30809	5.68707
90	4.39165	4.70723	5.03783	5.37977
100	4.20394	4.49336	4.79504	5.10552
110	4.03237	4.29900	4.57568	4.85919
120	3.87494	4.12156	4.37648	4.63668
130	3.72993	3.95890	4.19474	4.43465
140	3.59592	3.80922	4.02823	4.25035
	B10			
0.1	7.33483	8.26828	9.32096	10.48672
10	6.80990	7.60755	8.49014	9.44723
20	6.35397	7.04369	7.79480	8.59544
30	5.95785	6.56113	7.20938	7.89066
40	5.61037	6.14327	6.70945	7.29748
50	5.30298	5.77778	6.27735	6.79103
60	5.02904	5.45527	5.89998	6.35339
70	4.78330	5.16849	5.56746	5.97125
80	4.56158	4.91175	5.27214	5.63457
90	4.36046	4.68051	5.00802	5.33559
100	4.17718	4.47109	4.77036	5.06823
110	4.00942	4.28050	4.55532	4.82768
120	3.85528	4.10629	4.35976	4.61003
130	3.71312	3.94641	4.18113	4.41213
140	3.58160	3.79912	4.01729	4.23136

4. Conclusions

The density of a biodiesel produced from waste cooking oil and of two of its diesel blends was experimentally investigated over broad ranges of pressure and temperature. To the best of our knowledge, this is the first set of experimental data provided for waste cooking oil biodiesel in similar pressure and temperature ranges.

The main conclusions can be depicted as follows:

- The WCO biodiesel demonstrated high stability as well as suitable cold properties. This is due to its FAMES profile.
- The density value is somewhat higher than the allowed standards. At 293.15 (K) and for high pressures (120–140 MPa), the density seems to be affected by the high viscosity values of the biodiesel.
- Nevertheless, these first results obtained are very promising in view of its transferability at the industrial scale.
- This original set of experimental data measured for waste cooking oil biodiesel could be used to test predictive models developed for biodiesel thermodynamic properties.

Author Contributions: D.B. and T.X.N. conceived and designed the experiments; T.X.N. and J.-P.B. performed the experiments and analyzed the data; D.B. and T.X.N. wrote the paper.

Conflicts of Interest: The authors declare no conflict of interest.

References

1. Lin, L.; Cunshan, Z.; Vittayapadung, S.; Xiangqian, S.; Mingdong, D. Opportunities and challenges for biodiesel fuel. *Appl. Energy* **2011**, *88*, 1020–1031. [[CrossRef](#)]
2. Balat, M. Potential alternatives to edible oils for biodiesel production—A review of current work. *Energy Convers. Manag.* **2011**, *52*, 1479–1492. [[CrossRef](#)]
3. Bhuiya, M.M.K.; Rasul, M.G.; Khana, M.M.K.; Ashwath, N.; Azada, A.K.; Hazrata, M.A. Second Generation Biodiesel: Potential Alternative to Edible Oil-Derived Biodiesel. *Energy Procedia* **2014**, *61*, 1969–1972. [[CrossRef](#)]
4. Kalam, M.A.; Masjuki, H.H.; Jayed, M.H.; Liaquat, A.M. Emission and performance characteristics of an indirect ignition diesel engine fuelled with waste cooking oil. *Energy* **2011**, *36*, 397–402. [[CrossRef](#)]
5. Karmee, S.K.; Patria, R.D.; Ki Lin, C.S. Techno-Economic Evaluation of Biodiesel Production from Waste Cooking Oil -A Case Study of Hong Kong. *Int. J. Mol. Sci.* **2015**, *16*, 4362–4371. [[CrossRef](#)] [[PubMed](#)]
6. Montefrio, M.J.F.; Obbard, J.P. The economics of biodiesel derived from waste cooking oil in the Philippines. *Energy Sources Part B* **2010**, *5*, 337–347. [[CrossRef](#)]
7. Nas, B.; Berktaş, A. Energy potential of biodiesel generated from waste cooking oil: An environmental approach. *Energy Sources Part B* **2007**, *2*, 63–71. [[CrossRef](#)]
8. Sheinbaum-Pard, O.C.; Calderon-Irazoque, A. Ramirez-Suarez, M. Potential of biodiesel from waste cooking oil in Mexico. *Biomass Bioenergy* **2013**, *56*, 230–238. [[CrossRef](#)]
9. Man, K.L.; Keat, T.L.; Abdul Rahman, M. Homogeneous, heterogeneous and enzymatic catalysis for transesterification of high free fatty acid oil (waste cooking oil) to biodiesel: A review. *Biotechnol. Adv.* **2010**, *28*, 500–518.
10. Chhetri, A.B.; Watts, K.C.; Islam, M.R. Waste Cooking Oil as an Alternate Feedstock for Biodiesel Production. *Energies* **2008**, *1*, 3–18. [[CrossRef](#)]
11. Ndiaye, E.H.I.; Bazile, J.P.; Nasri, D.; Boned, C.; Daridon, J.L. High pressure thermophysical characterization of fuel used for testing and calibrating diesel injection systems. *Fuel* **2012**, *98*, 288–294. [[CrossRef](#)]
12. Fahd, M.E.A.; Lee, P.S.; Chou, S.K.; Wenming, Y.; Yap, C. Experimental study and empirical correlation development of fuel properties of waste cooking palm biodiesel and its diesel blends at elevated temperatures. *Renew. Energy* **2014**, *68*, 282–288. [[CrossRef](#)]
13. Yoon, S.H.; Park, S.H.; Lee, C.S. Experimental investigation of the fuel properties of biodiesel and its blends at various temperatures. *Energy Fuel* **2008**, *22*, 652–656. [[CrossRef](#)]
14. Uzun, B.B.; Kılıç, M.; Özbay, N.; Pütün, A.E.; Pütün, E. Biodiesel production from waste frying oils: Optimization of reaction parameters and determination of fuel properties. *Energy* **2012**, *44*, 347–351. [[CrossRef](#)]
15. Lagourette, B.; Boned, C.; Saint-Guirons, H.; Xans, P.; Zou, H. Densimeter calibration method versus temperature and pressure. *Meas. Sci. Technol.* **1992**, *3*, 699–703. [[CrossRef](#)]

16. Miyake, Y.; Baylaucq, A.; Plantier, F.; Bessières, D.; Ushiki, H.; Boned, C. High-Pressure (up to 140MPa) density and derivative properties of some amines (Pentyl-, Hexyl- and Heptyl-amines) between (293.15 and 353.15) K. *J. Chem. Thermodyn.* **2008**, *40*, 836–845. [[CrossRef](#)]
17. Pineiro, M.M.; Bessieres, D.; Gacio, J.M.; Saint-Guirons, H.; Legido, J.L. Determination of high-pressure liquid density for n-perfluorohexane and n-perfluorononane. *Fluid Phase Equilib.* **2004**, *220*, 127–136. [[CrossRef](#)]
18. Leung, D.Y.C.; Guo, Y. Transesterification of neat and used frying oil: Optimization for biodiesel production. *Fuel Process. Technol.* **2006**, *87*, 883–890. [[CrossRef](#)]
19. Sanli, H.; Canakci, M.; Alptekin, E. Predicting the higher heating values of waste frying oils as potential biodiesel feedstock. *Fuel* **2014**, *115*, 850–854. [[CrossRef](#)]
20. Knothe, G. “Designer” Biodiesel: Optimizing Fatty Ester Composition to Improve Fuel Properties. *Energy Fuels* **2008**, *22*, 1358–1364. [[CrossRef](#)]
21. Fu, J.; Hue, B.T.B.; Turn, S.Q. Oxidation stability of biodiesel derived from waste cat fish oil. *Fuel* **2017**, *202*, 455–463. [[CrossRef](#)]
22. Segovia, J.J.; Fandiño, O.; López, E.R.; Lugo, L.; Martín, M.C.; Fernández, J. Automated densimetric system: Measurements and uncertainties for compressed fluids. *J. Chem. Thermodyn.* **2009**, *41*, 632–638. [[CrossRef](#)]
23. Troncoso, J.; Bessieres, D.; Cerdeirina, C.A.; Carballo, E.; Romani, L. Automated measuring device of (p,rho,T) data-Application to the 1-hexanol plus n-hexane system. *Fluid Phase Equilib.* **2003**, *208*, 241–254. [[CrossRef](#)]
24. Troncoso, J.; Bessieres, D.; Cerdeirina, C.A.; Carballo, E.; Romani, L. P rho Tx data for the dimethyl carbonate plus decane system. *J. Chem. Eng. Data* **2004**, *49*, 923–927. [[CrossRef](#)]



© 2018 by the authors. Licensee MDPI, Basel, Switzerland. This article is an open access article distributed under the terms and conditions of the Creative Commons Attribution (CC BY) license (<http://creativecommons.org/licenses/by/4.0/>).